35.4: Three-Dimensional Optical Analyses of Fringing Effect in Small Color Pixels

B. L. Zhang, H. J. Peng, H. C. Huang and H. S. Kwok
Centre for Display Research, Hong Kong University of Science and Technology, Clear Water Bay, Kowloon, Hong Kong, China

Abstract

We present a three-dimensional optical analysis of fringing effect in small color pixels. In addition to the simulation of optical reflectance in visible spectrum, we further expressed the reflectance in spatial color. Color leakage was easily located and it agreed well with the experiments.

1. Introduction

We have developed a novel but practical color liquid-crystal-on-silicon (LCOS) microdisplay that integrated color filters on silicon as illustrated in Figure 1. The projection optics is greatly simplified since color is already available on the display. What it needs is just a polarizing beam splitter (PBS) to direct a polarized light into the display and back to a projection lens. In order to have high resolution for this spatial color microdisplay, pixels have to be very small. This is not a problem for silicon panels, which were fabricated by sub-micron very large-scale integration (VLSI) processes. But the lateral field effect among small color pixels could be severe [1-3], and degrade contrast and color of this microdisplay.

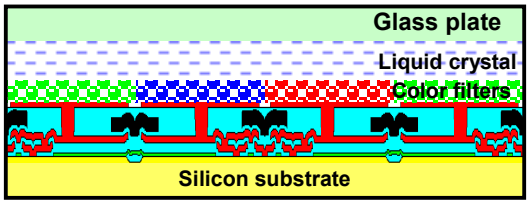

Figure 1 Schematic of color filter LCOS microdisplay

In this paper, we present a three-dimensional (3D) optical analysis of fringing effect in small color pixels. In our previous works, we have developed a two-dimensional (2D) optical modeling of small pixels in reflective twisted nematic cells [1]. In this work, we further included color filters in the simulation structures and elaborated the 2D modeling to three dimensions. The 3D optical analysis started with a numerical calculation of liquid crystal (LC) director in rectangular mesh. Thereafter we calculated for optical reflectance of color pixels in the visible spectrum by extended Jones matrix. The reflectance spectrum was then converted to the CIE 1931 color space for color coordinates. We further expressed the optical reflectance in standard RGB bitmap format, so we were able to visualize the color fringing effects among small color pixels. With this analysis as a tool, we are able to minimize the color fringing effect and optimize the display performance.

2. Characterization of Color Filters

There are four color filter manufacturing methods, which are electro-deposition, printing, dying and pigment dispersion. Pigment dispersed color filters were used in this color filter microdisplay for high resolution and light stability concerns. We modeled the color filters by an equivalent circuit of a resistor and a capacitor in parallel and measured their values by an LCR meter. With these two values, we proceeded to calculate for their dielectric constants, which were 4.63, 6.01 and 4.52, respectively, for red, green and blue color filters.

For optical parameters, we firstly used spectroscopic ellipsometer to measure optical reflectance of the color filters [4, 5]. The refractive index, n, and extinction coefficient, k, of color filters in transparent or near transparent region can be described by Cauchy dispersion formula as follows:

$$n(\lambda) = A_n + B_n/\lambda^2 + C_n/\lambda^4 \quad (1)$$

$$k(\lambda) = A_k + B_k/\lambda^2 + C_k/\lambda^4 , \quad (2)$$

where A_n, B_n, C_n, A_k, B_k and C_k are Cauchy coefficients. The color filter thickness d and the corresponding n, k values in the transparent region can be determined by the measured optical reflectance. Thereafter, the optical constants in the absorptive region can be obtained with known film thickness d. Figure 2 shows the measured and derived optical constants of color filters in the visible spectrum.

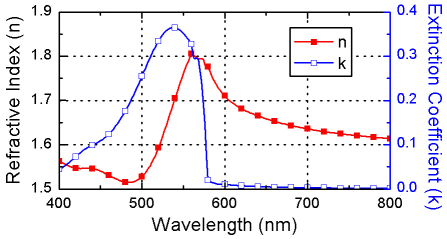

(a)

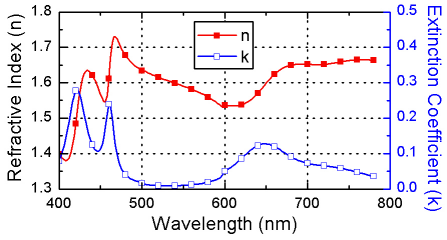

(b)

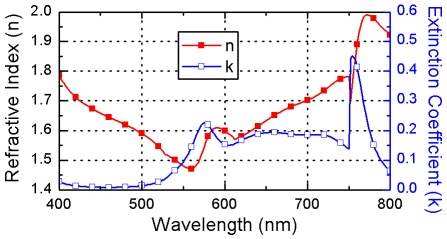

(c)

Figure 2 Optical constants of (a) red, (b) green and (c) blue color filters

 ISSN/0005-0966X/05/3602-1302-$1.00+.00

3. 3D Optical Analysis

3.1 LC Electro-mechanical Analysis

With dielectric constants of color filters available, we were able to analyze the electro-mechanical properties of color LC cells. In this analysis, 3D director configurations were calculated by simultaneously solving the 3D Poisson and continuum equations. Periodic boundary conditions were applied on both the left and right edges, at which the director, potential, and their derivatives were continuous. Figure 3 shows cross section of the 3D director distributions of monochrome and color pixels, in which the adjacent pixels had opposite driving polarity. SCTN mode [6] was used in this simulation, where the cell gap was 3.1μm and the LC mixture had a retardation of 0.1. Since the applied voltage was partially dropped in the color filters, the lateral electrical field extended more into the color pixels compared with the monochrome one. This implied that the color pixels had a more severe fringing effect.

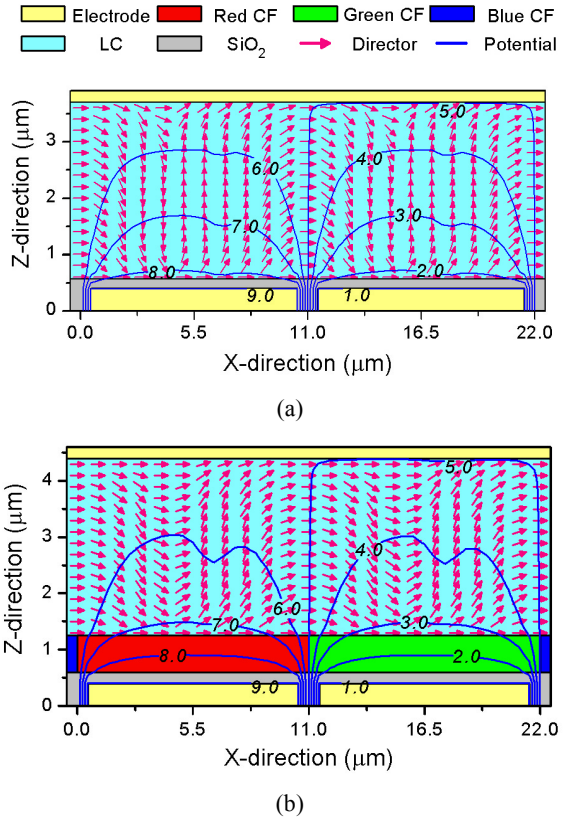

Figure 3 LC directors and fringing field in (a) monochrome and (b) color pixels

3.2 Optical Reflectance Analysis

With LC directors and optical constants of color filters available, we continued to calculate for optical reflectance of color pixels in the visible spectrum by extended Jones matrix [7]. We modeled the reflective color pixels by a transmittive LC cell, color filters and a mirrored transmittive LC cell of the first one in series as shown in Figure 4. The LC cells were treated as a stack of uniaxial and isotropic media. The color filters were represented by absorptive and isotropic media. The optical reflectance was calculated as the ratio of output over input intensity.

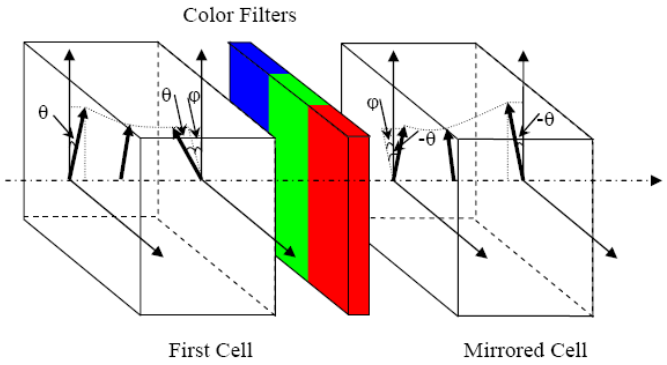

Figure 4 Simulation structures of the reflective color pixels

We arranged the color pixel array in delta shape and turned on the green pixels as shown in Figure 5(a). The common voltage remained at 5V. The sub-pixel was 11.2μm by 8.4μm for a pixel pitch of 16.8μm. We illuminated a 550nm light into this pixel array and calculated for its optical reflectance. Figure 5(b) shows contour of the simulated optical reflectance of the pixel array. The total optical reflectance at this wavelength could also be obtained by integrating the reflectance over the pixel array.

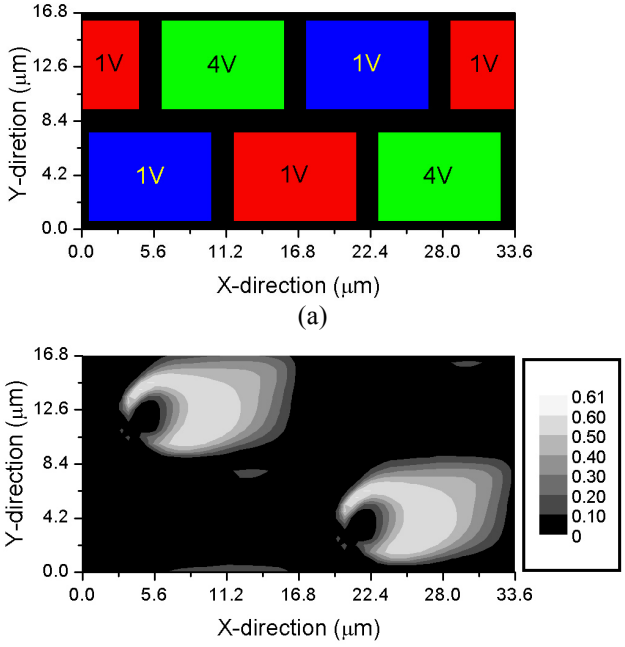

Figure 5 (a) Simulation structure and (b) optical reflectance contour of a color pixel array

We varied the wavelength of the illuminating light for the visible spectrum, and integrated the optical reflectance over this pixel array. Figure 6 shows the simulated optical reflectance in the visible spectrum. We have fabricated a color filter microdisplay of the same pixel size and LC mode. Figure 6 also shows the measured optical reflectance of this microdisplay by a spectro radiometer. The measurements were performed under a long-focus microscope with red, green and blue LED light sources. For a fair comparison, we also used these LED sources for the calculation of the optical reflectance. The simulated and measured optical reflectance agreed each other very well.

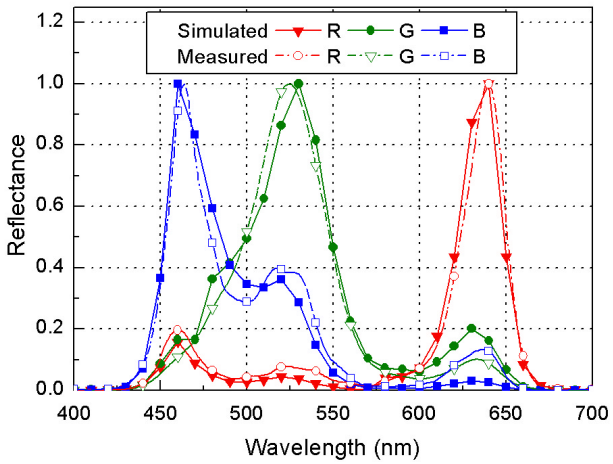

Figure 6 Measured and simulated optical reflectance

3.3 sRGB Representation of Color Pixels

The optical reflectance was then converted to the CIE 1931 color space for color coordinates, which was a good measure of color purity. But it lacked spatial information to illustrate which part of the pixels caused leakage and degraded the color. We further expressed the color coordinates in standard RGB bitmap format proposed by Hewlett-Packard and Microsoft [8], so we were able to visualize the color fringing effects among small color pixels. Figure 7 shows the observed and simulated color pixels of a SCTN mode microdisplay. The simulated spatial color images matched the observed ones very well. The leakage of dark pixels occurred on 4 sides of the dark pixels, but mainly on the left of bright pixels. The bright pixels were fully on and there was no dark spot within the bright pixels.

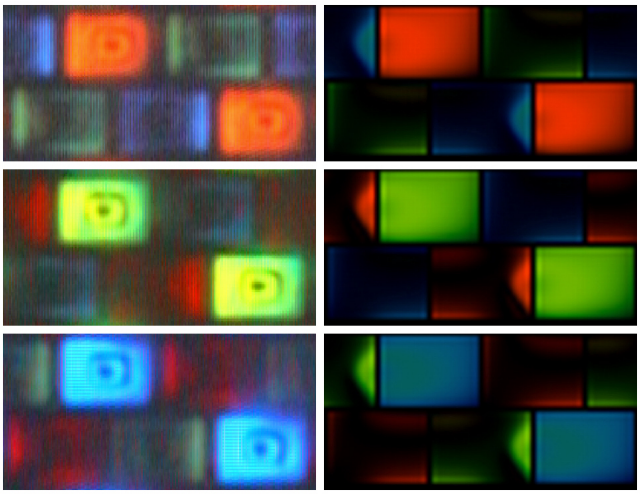

(a) (b)

Figure 7 (a) Observed and (b) simulated color pixels

4. Optimizations

With this 3D optical analysis as a tool, we were able to locate the leakage and minimize the color fringing effect. Arrangement of sub-pixels in stripe, delta or mosaic shapes would disperse the fringing field in different extents. Change of rubbing directions could move the leakage around. Alternating thickness or dielectric constant of color filters would re-distribute the electric field. But the most important design parameter is still on application specific LC modes. The color leakage could be minimized at a particular LC mode even at very small pixel size. In this section, we compared the color fringing effect in small color pixels by pixel arrangement, rubbing direction, LC mode and pixel size.

4.1 Pixel Arrangement

We arranged color pixels in strip and delta shapes and performed 3D optical analyses of these two structures. Both the structure used the same MTN mode [9] and had a same pixel pitch of 15μm. Figure 8 shows the spatial reflectance of both the pixel arrangements in which green pixels were turned on. The leakage occurred more on the blue pixels than in the red pixels in these pixel arrangements. However, it is clearly shown in the figure that the strip pixels had more leakage than the delta pixels. The color leakage extended almost 30% into the dark blue pixels in stripe pixel arrangement. As a result, the color purity of the strip pixels was much worse than that of the delta pixels. We obtained a green color purity of (0.223, 0.492) for the strip pixels and (0.241, 0.560) for the delta pixels. In addition to better color purity, the delta pixels had a larger feature size and hence easier for micro-color-filter processing.

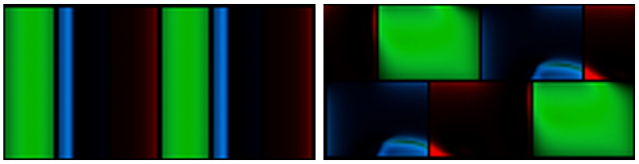

(a) (b)

Figure 8 Spatial optical reflectance of (a) strip and (b) delta pixels when green pixel were turned on

4.2 Rubbing Direction

The rectangular or square pixels had finite area and pixel edges. Rubbing direction with respect to the pixel edges could produce different degree of color leakage in the finite pixel area. There should be an optimized rubbing direction that would result in a least color leakage. However, the rubbing direction had to be related to the optical axis of the light path and could not be any arbitrary angle. It was only possible to rotate the rubbing angle by 90° and moved the color leakage to the short side of the pixels. Figure 9 shows the spatial optical reflectance of the same delta pixels in Figure 8 with two rubbing directions. Figure 9(a) had the color leakage penetrated more on the long side of dark pixels, while Figure 9(b) had the color leakage penetrated more on the short side of the dark pixels. It was found that the green color purity could be further improved from (0.241, 0.560) to (0.247, 0.585) when the color leakage was moved to the short side of the dark pixels.

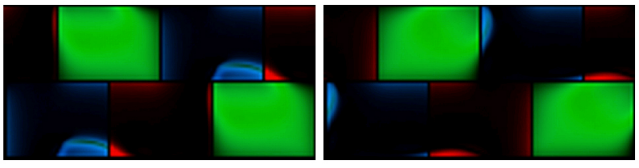

(a) (b)

Figure 9 Spatial optical reflectance with color leakage occurred on (a) long and (b) short side of pixels

4.3 Liquid Crystal Mode

In addition to SCTN and MTN modes, there are other mixed twisted nematic and birefrigence (MTB) modes [10] that are suitable for microdisplay applications. We did a systematic search of these MTB modes and found some modes that had very low color leakage. Figure 10 shows a comparison of the optimized MTN mode and the low-leakage MTB mode. The green color purity was further improved from (0.247, 0.585) of the MTN mode to (0.243, 0.601) of the low-leakage MTB mode. However, it should be noted that the on region in the green pixels of this MTB mode was also reduced to a smaller area.

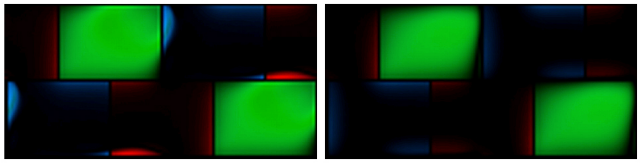

(a) (b)

Figure 10 Spatial optical reflectance of (a) MTN and (b) MTB modes

4.4 Pixel Size

In order to have high resolution for this spatial color microdisplay, pixels have to be very small. We further studied the color fringing effect with respect to the pixel size. Figure 11 shows the spatial optical reflectance of small pixels of 9 and 12μm. The color leakage was still insignificant. The green color purity was slightly reduced from (0.243, 0.601) of 15μm pixels to (0.233, 0.587) of 12μm, and to (0.231, 0.577) of 9μm pixels. But the on region in the green pixels was further reduced to a smaller area. This reduction in the bright pixels would not affect the overall light luminance, but would reduce individual color brightness.

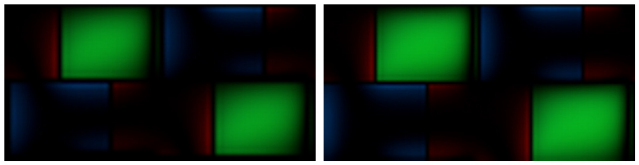

(a) (b)

Figure 11 Spatial optical reflectance of (a) 9μm and (b) 12μm pixels

5. Conclusions

We present a 3D optical analysis of fringing effect in small color pixels. We expressed the simulated optical reflectance in both the color coordinates and spatial color, so it was easier to quantify and locate the color leakage. The simulated optical reflectance agreed well with the experimental ones. With this 3D optical analysis as a tool, we further optimized color pixels with respect to pixel arrangement, rubbing direction, LC mode and pixel size. It was found that the color pixels could still maintain good color purity for pixel size less than 10μm with an optimized and application specific LC mode. This implies that this simple but novel color filter LCOS microdisplay technology is suitable for high-resolution display applications.

6. Acknowledgements

This work is supported partly by the Research Grant Council of the Government of the Hong Kong Special Administrative Region.

7. References

[1] H. C. Huang, D. D. Huang and J. Chen, “Two-dimensional optical analysis of small pixels in reflective silicon microdisplay”, Jpn. J. Appl. Phys. Vol. 39, p.485 (2000).

[2] K. C. Ho and M. Lu, “Study of the dynamics of the disclinations of reflective TN-LCDs by using a high-resolution digital camera”, SID’99, p.746, (1999).

[3] Y. Ji, J. Gandhi and M. E. Stefanov, “Fringe-field effects in reflective CMOS LCD design optimization”, SID’99, p.750, (1999).

[4] C. Defranoux, J. P. Piel, J. L. Stehle, “Spectroscopic ellipsometry and photometry applied to color filter characterization”, Int. Soc. Opt. Eng. Proceedings of Spie, Vol. 2873, p.184, (1996).

[5] F. Stern, “Dispersion of the index of refraction near the absorption edge of semiconductors”, Phys. Rev. 133, p. A1653 (1964).

[6] K. H. Yang, “A self-compensated twisted nematic mode for reflective light valves”, Euro Display ’96, p.499, (1996).

[7] Gu. C, Pochi Yeh, “Extended Jones matrix method II”, J. Opt. Soc. Am. A, Vol. 10, p.966 (1993).

[8] Refer to http://www.color.org/sRGB.html.

[9] S. T. Wu and C. S. Wu, “Mixed-mode twisted nematic liquid crystal cells for reflective displays”, Appl. Phys. Lett., Vol. 68, p.1455, (1996).

[10] J. Chen, P. W. Cheng, S. K. Kwok, C.S. Li, Steve Young,H.C.Huang and H.S.Kwok, Generalized mixed mode reflective liquid crystal displays for three-panel color projection applications, SID '99, p.754 (1999).